Crystal Structures of *Helicobacter pylori* Type II Dehydroquinase Inhibitor Complexes: New Directions for Inhibitor Design

David A. Robinson,[†] Kirsty A. Stewart,[‡] Nicholas C. Price,[†] Peter A. Chalk,[§] John R. Coggins,[†] and Adrian J. Lapthorn*[,‡]

Division of Biochemistry and Molecular Biology, Institute of Biomedical and Life Sciences, and Department of Chemistry, University of Glasgow, Glasgow G12 8QQ, Scotland, U.K., and GlaxoSmithKline, Medicines Research Centre, Gunnels Wood Road, Stevenage, Herts SG1 2NY, U.K.

Received June 7, 2005

The crystal structures of the type II dehydroquinase (DHQase) from *Helicobacter pylori* in complex with three competitive inhibitors have been determined. The inhibitors are the substrate analogue 2,3-anhydroquinate (FA1), citrate, and an oxoxanthene sulfonamide derivative (AH9095). Despite the very different chemical nature of the inhibitors, in each case the primary point of interaction with the enzyme is via the residues that bind the C1 functionalities of the substrate, 3-dehydroquinate, i.e., N76, H102, I103, and H104. The DHQase/AH9095 complex crystal structure shows that sulfonamides can form a scaffold for nonsubstrate-like inhibitors and identifies a large conserved hydrophobic patch at the entrance to the active site as a locus that can be exploited in the development of new ligands.

Introduction

The enzyme 3-dehydroquinate dehydratase (dehydroquinase, DHQase; EC 4.2.1.10) catalyses the reversible dehydration of 3-dehydroquinate to form 3-dehydroshikimate (Scheme 1), a reaction common to the biosynthetic shikimate pathway and the catabolic quinate pathway. The shikimate (pre-chorismate) pathway presents an ideal target for the development of novel antimicrobial agents, as it is present in bacteria, fungi, plants, and apicomplexan parasites but not present in mammals.[1−3] The importance of the pathway in bacteria is highlighted by the use of disruption mutants of typically *aroA* (EPSP synthase) and *aroD* (type I dehydroquinase) (produced in the presence of suitable media supplements) as attenuated live vaccines in a number of pathogenic bacteria such as *Salmonella typhimurium*[4] and *Bacillus anthracis*.[5] The attenuation of the bacteria is thought to be the result of depletion of folic acid of which the *p*-aminobenzoic acid (PABA) is derived from the shikimate pathway. Disruption of *aroQ* (type II dehydroquinase) in *Corynebacterium pseudotuberculosis* was more problematic, showing reduced growth *in vitro* (in complex media) and loss of virulence.[6] However, in *Mycobacterium tuberculosis*, the construction of viable *aro* gene disruption mutants has proved to be unsuccessful and has been attributed in part to the slow growth of mycobacteria. Recently, Parish and Stoker have successfully disrupted *aroK*, the gene for shikimate kinase, and shown it to be essential for viability of the organism, even in the presence of media supplements.[7] They propose, therefore, that the shikimate pathway is essential for the viability of *M. tuberculosis.*

Two structurally and mechanistically distinct forms of dehydroquinase, the third enzyme in the shikimate pathway, have been characterized.[8−10] This presents a significant opportunity for the development of selective antimicrobials. The type I enzymes are typically of monomer mass ∼25 kDa and active as homodimers, each monomer possessing an $(\alpha/\beta)_8$ fold similar to that of triose phosphate isomerase. The reaction catalyzed by the type I enzyme is a *syn* elimination of water, proceeding via an imine (Schiff base) intermediate, formed with a lysine residue within the active site.[11]

Scheme 1. Reaction Catalyzed by Type II Dehydroquinase Together with the Structures of **1** the Transition State Analogue 2,3-Anhydroquinic Acid (FA1, **1**), Citrate (**2**), and *N*-Tetrazol-5-yl-9-oxo-9*H*-xanthene-2-sulfonamide (AH9095, **3**) Identified from Compound Library Screening

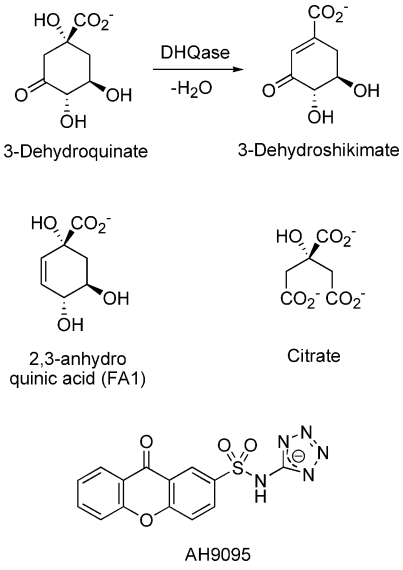

The monomers of the type II enzymes are smaller (approximately 16 kDa) and possess a flavodoxin-like fold; the enzymes are active as dodecamers. The type II reaction has been shown to proceed via an enol/enolate intermediate, resulting in *anti* elimination of water.[12] Type I enzymes are found in plants, fungi, archaea, and bacteria exclusively associated with the shikimate pathway, while the type II enzymes operate in both the shikimate pathway and the catabolic quinate pathway and are found in fungi and bacteria.

On the basis of the proposed catalytic mechanisms, selective inhibitors of type I and II DHQase have been developed from transition state analogues.[13−15] The inhibitor 2,3-anhydroquinic

* To whom correspondence should be addressed. Tel.: 0141-330-5940. Fax: 0141-330-4888. E-mail: adrian@chem.gla.ac.uk.
[†] Division of Biochemistry and Molecular Biology, University of Glasgow.
[‡] Department of Chemistry, University of Glasgow.
[§] GlaxoSmithKline.

10.1021/jm0505361 CCC: $33.50
Published on Web 02/02/2006

acid (FA1, Scheme 1) **1** was identified as a generic inhibitor of type II DHQase, whereas the ligand 3-dehydroquinate-*E*-oxime showed selectivity between type II DHQases from different species. Both inhibitors showed low micromolar inhibition of the type II enzymes while they were millimolar inhibitors of the type I enzyme.

Crystal structures of several type II inhibitors complexes with DHQases have been elucidated from *Streptomyces coelicolor*[16,17] and *M. tuberculosis* (unpublished PDB codes 1H0R and 1H0S). The active site of the *S. coelicolor* DHQase in complex with **1** included both an ordered glycerol and tartrate molecule derived from the crystallization conditions (PDB code 1GU1). This structure, and in particular the glycerol binding site, which is 3.7 Å away from the inhibitor, has been the focus of attempts to combine these two ligand binding sites and therefore enhance the inhibition of a series of second-generation compounds.[18,19]

To further understand the extent of the binding pocket for design of type II DHQases inhibitors, we have turned our attention to the enzyme from *Helicobacter pylori. H. pylori* is a slow-growing bacterium found in the gastric mucous layer or attached to the epithelial lining of the stomach. The bacterium has been shown to be the causative agent of more than 90% of duodenal ulcers and up to 80% of gastric ulcers. A crystal structure of the type II DHQase from *H. pylori* has recently been reported (PDB code 1J2Y)[20] showing the enzyme to have the same folded structure as the previously described type II enzymes. Disruption of dehydroquinase in *H. pylori* results in severely impaired growth even in complex media (C. L. Clayton, personal communication).

Type II dehydroquinase inhibitors might have potential use as novel antibiotics for human therapy, as they would be expected to have a restricted spectrum of antimicrobial activity to those human pathogens expressing the type II enzyme such as *H. pylori* and *M. tuberculosis*. A high-throughput screen of some 150 000 compounds against purified recombinant type II dehydroquinase from *H. pylori* expressed in *Escherichia coli* was used as a starting point to identify novel type II dehydroquinase inhibitors. This provided approximately 100 chemical inhibitors giving more than 50% inhibition of *H. pylori* dehydroquinase enzyme activity at a concentration of 20 μg/mL and with little or no structural similarity to substrate. Surprisingly, none of these compounds had equivalent activity against the recombinant type II dehydroquinase from *M. tuberculosis*. Furthermore, none of these compounds had potent antimicrobial activity. We report here the crystal structure of one of these compounds, *N*-tetrazol-5-yl-9-oxo-9*H*-xanthene-2-sulfonamide (AH9095) (Scheme 1) **3** in complex with *H. pylori* DHQase to 1.5 Å resolution. This structure shows how sulfonamides can inhibit DHQases and identifies new regions of the active site that could be exploited in inhibitor design. In addition, we have solved the crystal structure of the type II DHQase from *H. pylori* in complex with **1** and reinterpreted the structure 1J2Y, identifying the ligand as citrate **2**. Comparison of the inhibition of *H. pylori*, *S. coelicolor*, and *M. tuberculosis* type II DHQases by the three ligands is reported and the structural basis of ligand specificity discussed.

Results

Kinetic Analysis. The effects of the inhibitors **1**−**3** on type II DHQases are summarized in Table 2. All three ligands showed competitive inhibition toward the type II DHQases from *S. coelicolor* and *H. pylori*. The inhibition of *S. coelicolor* and *M. tuberculosis* DHQase by **1** has been characterized previously,[13] with the ligand showing 7-fold selectivity toward *S. coelicolor* DHQase over the *M. tuberculosis* enzyme (K_{EI} values of 30 μM and 200 μM respectively). In the case of *H. pylori* DHQase, FA1 was found to act as a competitive inhibitor with a K_{EI} of 370 μM. Compound **2** inhibited both *S. coelicolor* and *H. pylori* DHQases, albeit with relatively low affinity (the K_{EI} values were 7.3 and 2.5 mM, respectively). *M. tuberculosis* DHQase was not significantly inhibited by compound **2**, with less than 10% inhibition in the presence of 20 mM **2** at a substrate concentration of 200 μM. Compound **3** shows strong inhibition of *H. pylori* DHQase (K_{EI} = 20 μM), whereas against *S. coelicolor* DHQase the inhibition is an order of magnitude weaker (K_{EI} = 230 μM). This compound shows negligible inhibition of *M. tuberculosis* DHQase; thus, at a substrate concentration of 200 μM, there was less than 10% inhibition in the presence of 200 μM inhibitor.

Table 1. Crystallographic Data and Refinement Statistics

Details of Data Collection			
data set	AH9095	FA1	citrate[f]
wavelength (Å)	0.870	1.00	1.00
space group	*F*23	$P3_1$	$P4_232$
unit cell dimensions (Å)	$a = b = c =$ 131.37	$a = b =$ 103.9, $c =$ 217.5	$a = b = c =$ 98.9
resolution range (Å)	50.0−1.5	46.5−3.1	44.2−2.5
observations	334 701	145 663	239 220
unique reflections	27 302	43 824	6146
% completeness	100	90.4	100
R_{merge}[a] (%)	4.4	9.2	8.6

Refinement Statistics			
resolution range (Å)	30.0−1.55	25.0−3.1	30.0−2.5
R-factor[b] (R_{work}/R_{free})	15.6/19.3	20.7/23.7	17.00/21.16
number of atoms[c]	1165/40/177	14224/144/−	1227/13/40
rms bond length deviation (Å)	0.014	0.024	0.027
rms bond angle deviation (deg)	1.56	2.07	2.24
mean *B*-factor (Å)[d]	23/16/45	61/60/−	21/23/25/38
coordinate error (Å)[e]	0.0929	0.5105	0.2847

[a] $R_{merge} = \sum|I - \langle I\rangle|/\sum\langle I\rangle$. [b] *R* factor $= \sum|F_o - F_c|/\sum F_o$. [c] Number of atoms of protein, heteroatoms and water molecules, respectively. [d] Mean *B* factor for protein, inhibitor and water atoms, respectively. [e] Calculated using the method of Cruickshank.[38] [f] Statistics from ref 21; structure factors from PDB entry 1J2Y.

Table 2. Inhibition of Type II Dehydroquinases by Different Ligands[a]

DHQase	**1** (μM)	**2** (mM)	**3** (μM)	phosphate (mM)[b]
H. pylori	370± 50	2.5 ± 0.2	20 ± 3	9 ± 0.6
S. coelicolor	30 ± 10[c]	7.3 ± 0.9	230 ± 25	7 ± 0.6
M. tuberculosis	200 ± 20[c]	*d*	*e*	complex pattern

[a] The values shown are the K_{EI} values for the three inhibitors that show competitive inhibition with respect to the substrate, 3-dehydroquinate. The kinetic parameters for the three enzymes are as follows: *H. pylori*, k_{cat} = 1 s^{-1} and K_m = 205 μM; *S. coelicolor*, k_{cat} = 125 s^{-1} and K_m = 100 μM; and *M. tuberculosis*, k_{cat} = 5 s^{-1} and K_m = 24 μM, as reported in Evans et al.[23] [b] Data from Evans et al.[23] [c] Data from Frederickson et al.[13] [d] <10% inhibition observed upon addition of 20 mM ligand, at a substrate concentration of 200 μM. [e] <10% inhibition observed upon addition of 200 μM ligand, at a substrate concentration of 200 μM.

Whole Cell Inhibition Studies. The A_{595} measurements for native *E. coli*, the control growth experiments with minimal media and minimal media supplemented with 1 mM shikimate, showed equivalent values, which were used as the reference level of growth. The corresponding A_{595} measurements for *E. coli* strain AB2848 (-DHQase) with *H. pylori* DHQase-containing plasmid (pet19) showed a 20% decrease in absorbance with 50 μg/mL (0.145 mM) AH9095 compared to 100% of the reference level obtained when supplementing the media with shikimate. Of 30 compounds screened in this way, 17 showed some level of selective growth impairment, which could be removed by supplementing the media with shikimate. The

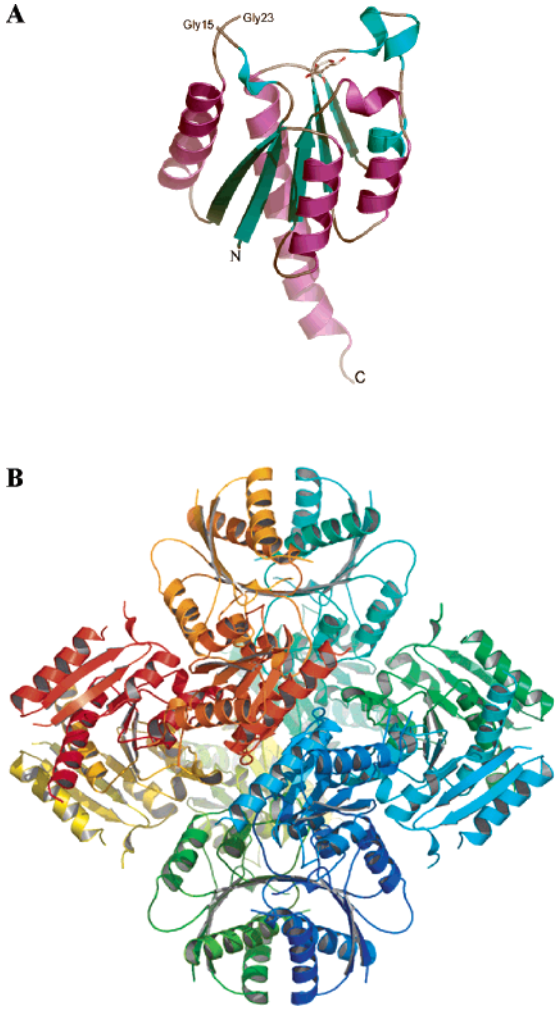

Figure 1. A ribbon representation of (A) the *H. pylori* DHQase−**1** structure colored according to secondary structure and the ligand represented as stick and colored according to atom type. (B) The dodecameric quaternary structure of *H. pylori* DHQase colored by monomer. Diagrams were produced using PyMol (DeLano, W. L. The PyMOL Molecular Graphics System (2002) DeLano Scientific, San Carlos, CA).

decrease in the levels of growth was modest in all cases and not greater than 30%.

Structure of *H. pylori* DHQase Complexes. The final refined models of the *H. pylori* type II DHQase−inhibitor complexes have the same folded structure, and the monomer has a flavodoxin type α/β fold, as seen in other type II DHQases[8,16] (Figure 1a). A particular distinction in the *H. pylori* DHQase structures is a C-terminal helix that is much longer than that observed in any other type II DHQase, extending 12 residues (3.5 turns) beyond the main body of the monomer. The quaternary structure is a dodecamer with 23 symmetry as seen for all type II DHQases; in the *H. pylori* DHQase−inhibitor **1** structure, a dodecamer is present in the asymmetric unit, while in the structures of the other two inhibitor complexes the dodecameric quaternary structure is generated from crystallographic symmetry (Figure 1b).

The structure of *H. pylori* DHQase−inhibitor **2** contains one monomer per asymmetric unit, and the protein chain extends from Met1 to Asn158 (residues 159−167 are not ordered in the structure) and is essentially identical with that described by Lee et al.[20] Several rounds of refinement and model building of this structure and reinterpretation of the active site ligand have resulted in a significantly improved structure. In comparison with the structure reported by Lee et al.,[20] both R_{work} and R_{free} have been improved by 4.8% and 6%, respectively, while in the refinement reported here all data to 2.5 Å resolution (6146 reflections) have been used, as opposed to data to 2.6 Å with an $I > 2\sigma$ cutoff (5133 reflections).

In the complexed structures of DHQase inhibitors **1** and **3**, the C-terminus is disordered and only visible to Asn158 and Glu153, respectively, while both have extended N-termini due to the presence of a 6xHis tag. The structure of DHQase−inhibitor **2** has an ordered catalytic lid loop, while in the DHQase−**1** complex residues 16−22 are not seen. The lid loop in the DHQase−**3** complex structure is disordered with only the main conformation modeled with occupancy 0.8 between residues 17 and 23 and side chains for Arg20 and Leu21 and Met24 not modeled. The lid loop in this structure adopts essentially the same conformation as the DHQase−**2** structure with the exception that Pro19 could not be fitted in the weak electron density as a *trans* proline. The xanthene ring of inhibitor **3** occupies the same space as the side chains of Arg17 and Tyr22 in the DHQase−**2** structure, and as a result, the lid loop is moved around 5 Å out of the active site by a hinged movement at residues Leu14 and Val25 in the DHQase−inhibitor **3** structure.

The protein used for crystallization in this work included an N-terminal 6xHis tag, which includes a thrombin cleavage site (additional N-terminal sequence MGSSHHHHHHSSGLVPRGSH) to aid purification. In contrast, the protein used by Kwak and co-workers was the native form of the enzyme.[21] In the DHQase−inhibitor **3** structure, 12 residues (numbered −11 to 0) of the N-terminal tag are visible as an extended structure. The chain is disordered between residues −3 and 1 and adopts two different main chain conformations. The tag makes crystal contacts with two subunits of a related dodecamer, lying across the dimer interface. In the DHQase−inhibitor **1** structure, which consists of a complete dodecamer, the tag appeared to be visible only to Ser−1. However, additional electron density was observed for chains A, D, G, and J, corresponding to residues from the N-terminal 6xHis tag and linker region (residues −18 to −9). Comparing these structures with the native structure of Kwak and co-workers[21] shows little evidence of any difference in the structures caused by the N-terminal tag. The kinetic properties of the N-terminally tagged enzyme ($k_{cat} = 0.9\ s^{-1}$, $K_m = 205\ \mu M$) were similar to those reported by Bottomley et al. [22] for the native enzyme ($k_{cat} = 2.0\ s^{-1}$, $K_m = 590\ \mu M$) under similar conditions. The differences between the two sets of values most likely arise from differences in the measurement of protein concentrations and the use of a more highly purified preparation of substrate.[23]

Ligand Binding. *H. pylori* DHQase interacts with **1** in a manner similar to the previously reported *S. coelicolor* complex [16] (Figure 2a). The carboxylate at the C1 position of the ligand forms four hydrogen bonds to the protein. Atom O1 interacts with the backbone N atom and the OG1 atom of Thr104 while atom O2 forms H-bonds with the backbone N atom of Leu103 and ND2 of Asn76. The C1 hydroxyl group forms two hydrogen bonds to the protein, with atom ND2 of His102 and with atom OD1 of Asn76. In addition to the hydrogen bonds formed at the C1, the hydroxyl group at C5 of the ligand hydrogen bonds with NH1 of Arg113 and NE2 of His82. In complex structures of **1** with *S. coelicolor* and *M. tuberculosis* DHQase, there is a further interaction between the C4 hydroxyl of FA1 and an active site aspartate residue. The distance between the O4 atom and the OD2 atom of Asp 89* in the *H. pylori* DHQase/FA1 inhibitor structure is 3.28 Å and does not appear to be as strong.

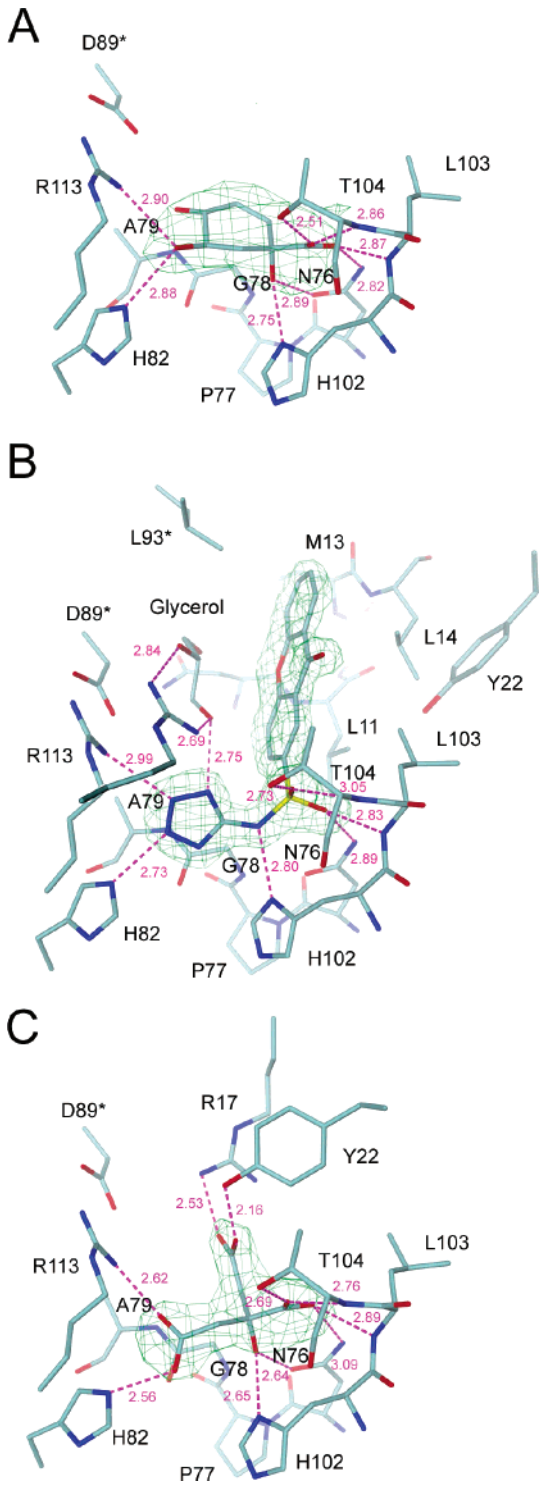

Figure 2. Detailed views of the active sites of the three *H. pylori* DHQase/inhibitor crystal structures, namely DHQase in complex with (a) **1**, (b) **3** with glycerol, and (c) **2**, with key amino acid residues represented in stick, labeled, and colored by atom type. Hydrogen bonds between the inhibitor and protein ≤3.2 Å in length are shown as dashed lines colored magenta and labeled. Difference electron density was calculated after one round of refinement with all the active site waters and the ligand removed. This electron density is contoured between 1σ and 2σ difference density and represented as wire mesh and colored green. This diagram and Figure 3 were produced using DINO (http://www.dino3d.org).

In the inhibitor **3**−DHQase structure the inhibitor occupies the ligand binding pocket and the entrance to the active site (Figure 2b). The sulfonamide moiety of the ligand makes five hydrogen bonds to the protein via main chain and side chain atoms. Atom O1 forms two H-bonds with the amide group ND2 of Asn76 and with the backbone N atom of Leu103, atom O2 forms hydrogen bonds with the OG1 atom and the backbone N atom of Thr104, and atom N4 interacts with the side chain of His102. Residues 102−105 form the H-X-S/T-N motif common to all type II dehydroquinases. These interactions are analogous to those formed between sulfate and phosphate ions with type II DHQases,[23] and more importantly they mimic the proposed interaction between the hydroxyl and carboxylate functionalities at the C1 position of the substrate and the protein.[16] It is noticeable that the atom N4 of the sulfonamide actually matches the position of the C1 carbon of inhibitors such as FA1 and substrate, and as a result, the imidazole ring of His 102 moves 0.7 Å via a 20° rotation of the side chain to form the favorable hydrogen bond. It would be expected that the His-Glu salt bridge with Glu100 would be broken; however, this side chain rotates to maintain the interaction. The only significant change in the structure accompanying this movement is that the side chain of Ser81 rotates 85° and adopts a new rotamer conformation.

The tetrazole moiety occupies the area of the active site where the main body of the substrate dehydroquinate has been shown to bind in *S. coelicolor* DHQase.[16] The tetrazole ring is smaller than dehydroquinate and lies perpendicular to the plane of dehydroquinate ring. H-bonds are formed between the conserved active site residues Arg113 and His82 to atoms N1 and N2 of **3**, respectively. Both these residues interact with the C5 hydroxyl of dehydroquinate, a group that has been shown to be critical for activity.[24] An additional H-bond is formed from atom N to a bound glycerol molecule from the cryoprotectant solution.

The oxoxanthene moiety of the ligand packs against the hydrophobic surface of the active site entrance. One face of the planar ring system packs against a flat surface formed by the side chains of Leu residues 11, 14, and 103. The other face of the ligand packs against main chain and side chain atoms from Asn10 and Met13 and against the side chain of Leu93* from a neighboring subunit. The glycerol molecule that hydrogen bonds to the tetrazole moiety also packs against this face of the inhibitor.

In the *H. pylori* DHQase−inhibitor **2** structure the ligand makes 10 hydrogen bonds to the active site of the enzyme, with every oxygen atom in the ligand making at least one contact with the protein (Figure 2c). The central carbon C3 of the citrate molecule has a hydroxyl (atom O7) and carboxylate group, which is equivalent to the chemical moieties at C1 of inhibitor **1**. As a result, these groups adopt the same conformation in complex with **2** as seen in **1**, fully coordinated to Asn76 and the H-X-S/T-N motif (102−105). In addition, the **2** comprises two acetate moieties bonded to the central carbon C3. One of these acetate moieties (acetate 1) forms two hydrogen bonds; one interacts with Arg113 (atom O1) and the second with His82 (atom O2). These interactions are equivalent to those formed by the C5 hydroxyl of **1**, although neither of the acetate 1 oxygen positions is coincident with the hydroxyl oxygen. The second acetate moiety (acetate 2) forms two hydrogen bonds with residues from the lid loop, one with Arg17 (atom O3) and a second short contact with the hydroxyl of Tyr22 (atom O4). The interactions made by acetate 2 do not correspond to any made with **1** or the substrate of the enzyme dehydroquinate.

Discussion

In this paper, we report the structure of the type II DHQase from *H. pylori* in complex with three different inhibitors, identified by random screening, rational design, and the

serendipity of crystallization. Despite the different chemical nature of each inhibitor, the primary point of interaction with the DHQase is via the residues that bind the C1 hydroxyl and carboxylate groups of the substrate, i.e., Asn76, His102, Leu103, Thr104.

In the *H. pylori* DHQase−**1** complex structure it is clear, within the margin of error associated with the resolution of the X-ray data, that the inhibitor interacts with the protein, as has been observed previously for other type II DHQases.[16] The inhibition constant K_{EI} of 370 μM determined for this inhibitor against the *H. pylori* DHQase shows that **1** is ∼5−10 times weaker an inhibitor of this enzyme than of the *S. coelicolor* and *Aspergillus nidulans* type II DHQases.[13] The *H. pylori* enzyme is similar to the low k_{cat} *M. tuberculosis* enzyme in this respect, which suggests that the active site of these enzymes is not optimized for transition state stabilization as in the high k_{cat} enzymes. An order of magnitude difference in K_m values between the two enzymes suggests that similarities between the two enzymes do not extend further; this is confirmed by the inhibition data for **2**, **3**, and phosphate (Table 2).

The discovery of **2** in the active site of the *H. pylori* DHQase structure reported by Lee et al.[20] was of interest due to the large number of hydrogen bonds formed between the ligand and the protein. Although not suitable itself as an inhibitor, the large number of favorable interactions suggested a potential template on which to build an effective inhibitor. The kinetic analysis of the inhibition of *H. pylori* DHQase by citrate shows it to be a weak millimolar competitive inhibitor of the enzyme, showing only 4-fold stronger inhibition than phosphate. **2** was no better an inhibitor of the *S. coelicolor* enzyme than phosphate and showed no inhibition of the *M. tuberculosis* DHQase. As **2** is a flexible molecule, there is an entropic penalty for binding to the active site of DHQase compared to phosphate; however, it would be expected that the favorable hydrogen bonding between inhibitor and protein would significantly offset this. Comparison of all three *H. pylori* DHQase−inhibitor structures reported here suggests further reasons for this disappointing level of inhibition by **2**. In particular, the carboxyl of the acetate 1 moiety binds in an unusual conformation in the plane of the C4−C5 bond of the FA1 ring and the oxygen positions do not coincide with either the C4 and C5 hydroxyls positions of the transition state analogue (Figure 3a). As a result, there is disruption in the position of the Arg113−Asp89* salt bridge, which moves ∼1 Å, and one of the two hydrogen bonds is lost. In addition, the imidazole ring of His82 is shifted by 0.5 Å, as is the main chain of residues between Gly78 and Ile87. These distortions to the protein permit the formation of two short hydrogen bonds (Figure 2c). The carboxylate of the acetate 2 moiety of the inhibitor forms hydrogen bonds with the side chains of the invariant residues of Tyr22 and Arg17 and thus closes the catalytic lid loop. It does not distort the active site in the same way as the acetate 1 moiety, although the hydrogen-bonding distances are not optimal and there is a short contact with the hydroxyl of Tyr22. The C4 atom of the acetate 2 moiety superimposes well with the C2 atom of **1**, suggesting that this is a possible branch for further investigation. It can be envisaged that the addition of a negatively charged branch from the C2 position could increase the potency of a new generation of transition state analogues of type II DHQases. Recent work investigating the addition of functional branches at the C1, C4, and C3 positions of transition state analogues[18,19] has shown moderate success, with nitrobenzyl derivatives at the C4 position acting as potent inhibitors. This strategy was given impetus by the identification of a tightly bound molecule of tartrate in a pocket near the active site of *S. coelicolor* DHQase.[16] Building on this approach, addition of groups at the C2 position would appear to provide promising lines for further derivatization, although this would present some significant synthetic challenges.

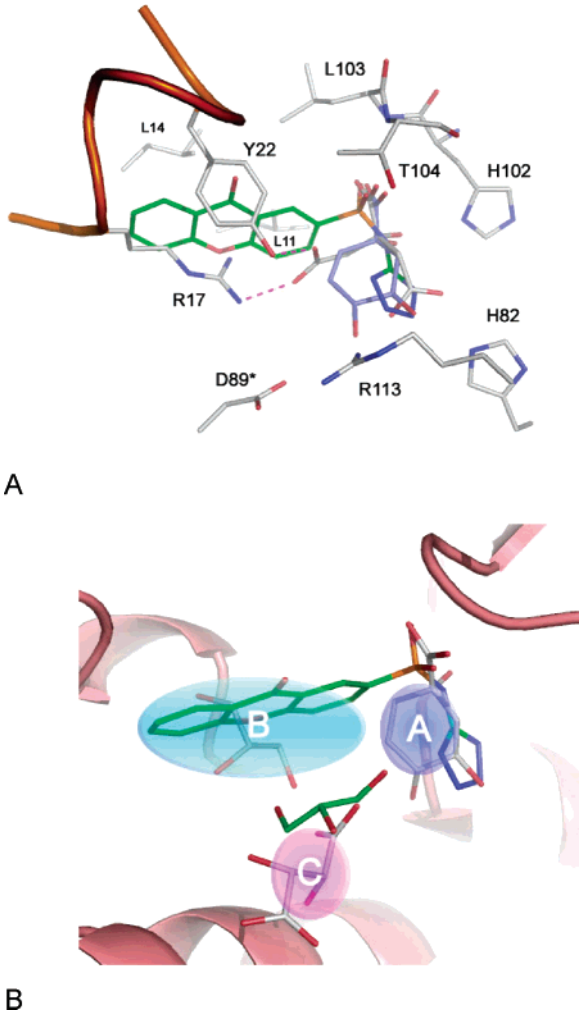

Figure 3. (a) The relative positions of the three inhibitors, within the *H. pylori* DHQase active site. The protein structure shown is that of the DHQase inhibitor **2** complex with interacting residues shown colored according to atom type (**1**, carbons colored purple; **2**, carbons colored gray; and **3**, carbons colored green for clarity). The main chain of the flexible lid domain, which is ordered in this structure, is shown in a ribbon colored orange. Hydrogen bonds between the citrate and the invariant arginine and tyrosine residues from the lid domain are shown in magenta. (b) A superposition of **3** with glycerol (atoms colored according to atom type, carbons green) and the *S. coelicolor* **1** inhibitor complex + tartrate and glycerol (pdb code 1GU1) (atoms colored according to atom type, carbons white). The *H. pylori* DHQase structure is shown in ribbon representation to delimit the active site. Three parts of the active site are highlighted according to the *S. coelicolor* structure, namely, A shows the core substrate binding pocket where **1** binds; B shows the glycerol pocket, which has been the focus of a series of second-generation inhibitors; and C shows the tartrate binding pocket.

Compound **3** is superficially similar in structure to the sulfonamide antibiotics, which are inhibitors of the enzyme dihydropteroate synthase and act by blocking folate biosynthesis. **3** has an oxoxanthene ring instead of the key *p*-aminobenzyl group of these antibiotics. The structure of the *H. pylori* DHQase inhibitor **3** complex illustrates how sulfonamides could form a basic template for the development of nonsubstrate-like type II DHQase inhibitors. The sulfonamide almost completely matches the hydrogen-bonding pattern of the functional groups at the

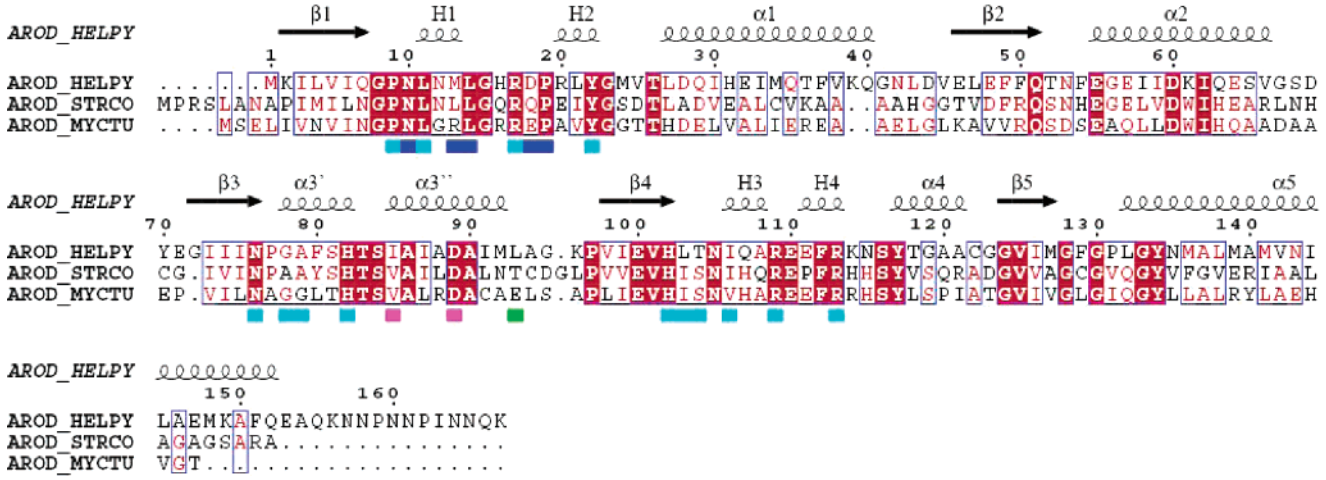

Figure 4. Sequence alignment of three type II DHQases with the secondary structure and numbering corresponding to the *H. pylori* structure. Boxed residues are partially conserved between sequences, and blocks of red highlight invariant residues between sequences. The amino acid residues with a bar beneath the alignment are contacted by the inhibitor molecules. Cyan represents common contacts made by compounds **1**−**3** (Arg17 and Tyr22 do not interact with **1**, as they are part of the disordered loop in this structure, but they are included anyway), while blue represents additional contacts made by **3**. Likewise, magenta represents common contacts made to the trimer-related subunit that closes the active site, while green represents the additional contact residue made with **3**. This diagram was produced using ClustalW[39] and ESPript[40].

C1 position of 3-dehydroquinate analogues; this is despite the absence of an atom in the position of the C1 hydroxyl. There is, therefore, no hydrogen bond to OD1 of Asn76; however, the N4 atom of the sulfonamide that occupies the same position as C1 still hydrogen bonds to the side chain of His 102 due to a rotation of this residue. Substituted bis-sulfonamides have been shown to act as inhibitors of type II DHQase and dehydroquinate synthase[25] with IC_{50} values in the low micromolar range. In this paper, we have used the *H. pylori* DHQase−**3** complex structure to show how at least one of the sulfonamide groups could interact with the active site of type II DHQases. With respect to the potential binding mode of sulfonamide ligands to dehydroquinate synthase (DHQS), the coordination of the substrate analogue carbaphosphonate bound to *Aspergillus nidulans* DHQS[26] (PDB code 1DQS) shows that the C1 carboxyl is coordinated by an arginine side chain, while the hydroxyl functionality is coordinated by an asparagine and a ordered water molecule. Some of the interactions can readily be mimicked by a sulfonamide group, as observed in the DHQase structure reported here; however, it is unclear how the N of the sulfonamide will hydrogen bond, as there is less scope for the movement seen in the DHQase structure in the DHQS active site.

The oxoxanthene ring of **3** makes extensive hydrophobic interactions with the *H. pylori* DHQase occupying a hydrophobic surface exposed when the lid loop is in the open position. Comparison with the *S. coelicolor* DHQase **1** inhibitor structure shows that the oxoxanthene ring occupies in part the same site as the ordered glycerol molecule in that structure (Figure 3b). The ring buries approximately 100 Å^2 of predominantly nonpolar surface accessible area in a segment between residues Pro9 and Tyr22. In addition, Leu93* from the symmetry-related monomer moves 2 Å, relative to other type II DHQase structures, to pack against the oxoxanthene ring.

The tetrazole is well-known as a carboxylate isostere and is used to improve permeability and cell penetration in a number of drugs, notably nonpeptidic angiotensin II type 1 receptor antagonists. **3** occupies the active site cavity of DHQase in an orientation perpendicular to that adopted by the ring of **1** (Figure 3a). The N1 and N2 atoms of the tetrazole moiety are positioned equidistantly from the position occupied by the C5 hydroxyl in the DHQase−inhibitor **1** structure and individually satisfy the hydrogen bonding of this group. The N of the tetrazole makes a hydrogen bond to a glycerol found within the active site (Figure 2a), which packs against the large oxoxanthene ring of the inhibitor. This part of the active site is clearly amenable to further chemical investigation, as simple analysis using LUDI (Accelrys, San Diego, CA) suggests that the hydroxyl of the glycerol can be joined via a single carbon bond to the position of the tetrazole. This glycerol forms two strong hydrogen bonds with the invariant Arg109 (which is implicated in the catalytic mechanism) and therefore would be desirable to include in the interactions made by the inhibitor. This glycerol binding site overlaps the previously identified tartrate binding pocket (Figure 3b),[16] which to date has not been fully exploited in inhibitor design.

Compound **3** is a competitive inhibitor of type II DHQases, shows 7-fold selectivity toward *H. pylori* DHQase over *S. coelicolor* DHQase, and no significant inhibition of *M. tuberculosis* DHQase. Sequence comparison of the three enzymes with the footprint of the three inhibitors highlighted (Figure 4) shows that the core inhibitor-binding site is highly conserved between the three enzymes. Superimposition of the *M. tuberculosis* DHQase, *S. coelicolor* DHQase, and *H. pylori* DHQase structures shows that there is very little difference in the active site topology between the enzymes. As stated previously, the primary site of protein−ligand interaction is with the highly conserved residue Asn76 and the conserved H-X-S/T segment (His102−Thr104); therefore, the stronger binding of **3** by *H. pylori* DHQase is intriguing.

The differences in inhibition of the *M. tuberculosis* enzyme are not well understood and can be considered as a special case. For example the inhibition by phosphate is complex, and a crystal structure in complex with sulfate shows that sulfate does not bind optimally in the active site, as seen in the *S.* coelicolor structure.[23] The absence of observable inhibition by citrate further supports the idea that the conserved H-X-S/T segment of the enzyme is not as significant for inhibitor binding.

If the entrances to the active site in the structures of DHQase from the three species are examined, differences that could influence ligand specificity are found. In the case of *H. pylori* DHQase, the tricyclic moiety of **3** sits against a relatively flat hydrophobic surface, packing against a series of Leu side chains (Figure 5a). In *M. tuberculosis* DHQase, this surface is less

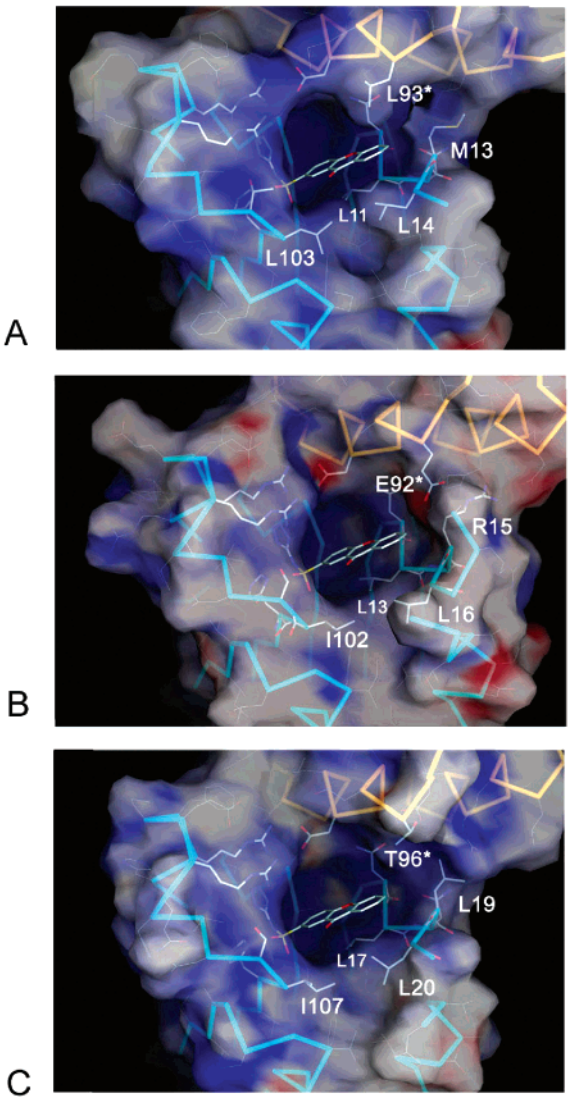

Figure 5. Views of the active site of (A) the *H. pylori* DHQase−inhibitor **3** complex, compared with DHQase structures from (B) *M. tuberculosis* and (C) *S. coelicolor* with **3** superimposed. A CA trace colored according to protein chain is shown for each protein structures, and important amino acid residues are highlighted in stick and colored according to atom type. A semitransparent surface is shown colored by electrostatic potential (blue, positive; red, negative).

complementary to the ligand, as one of the Leu side chains (Leu103) is replaced by an Ile (Ile102) and also favorable interactions made by Leu (Leu93* in the *H. pylori* enzyme) are no longer possible, since this is replaced by a Glu residue (Glu92*) (Figure 5b). This residue shows no conservation within type II DHQases, though generally it is a nonpolar residue. The presence of this charged patch upon the binding surface would repel the hydrophobic portion of **3**.

In the *S. coelicolor* DHQase (Figure 5c) there is a neutral residue (Thr96*) in this position, which would not contribute to the interactions with the inhibitor. The surface that packs against the lower face of the oxoxanthene moiety is exclusively hydrophobic but not as complementary to the planar ligand as seen in *H. pylori* DHQase. The differences in binding are probably due to a combination of effects. It is possible that the lid loop, which is more ordered in the *S. coelicolor* enzyme, interferes with the binding of **3** or that His102 (His 106) is not able to move and coordinate the sulfonamide, as occurs in the *H. pylori* structure, thus weakening the binding.

In the whole cell inhibition studies reported here, 50 μg/mL (0.145 mM) **3** weakly inhibits growth of an *E. coli* DHQase deficient strain complemented with the *H. pylori* DHQase. Supplementing the media with 1 mM shikimate restored growth to the control levels, suggesting that the inhibitor selectively acts on the type II DHQase. Given that the inhibition by **3** is competitive in nature with a K_{EI} of only 30 μM, it is probable that the buildup of substrate could overcome the inhibition rather than clearance of the compound by the bacteria. The development of more potent sulfonamide-based inhibitors should confirm this.

Taking these observations together, it is clear that there is significant scope for the generation of a range of nonsubstrate-like compounds that selectively inhibit type II DHQases from different species. The complex of *H. pylori* DHQase with **2** shows that there are additional H-bond partners within the active site which if optimized could improve potency. The complex with **3** indicates that sulfonamides can form a scaffold for nonsubstrate-like inhibitors. It also shows that a large hydrophobic surface at the entrance to the active site, which forms the binding surface for the invariant arginine and catalytic tyrosine, can be exploited in the development of new ligands. Designed inhibitors of type II DHQase have been small highly functionalized, hydrophilic compounds. The structure of the DHQase in complex with **3** shows that it is possible to add bulky nonpolar substituents to these compounds, thereby improving the membrane permeability, and hence the delivery, of potential inhibitors.

Experimental Section

Enzyme Purification. Type II DHQases from *H. pylori*, *M. tuberculosis*, and *S. coelicolor* were overexpressed and purified as described previously.[16,23] The protein was dialyzed into 10 mM Tris-HCl pH 7.0 and concentrated to 10 mg/mL using Centricon-50 centrifugal concentrators (Amicon). Stock solutions (100 mM) of the inhibitors **1** and **3** were prepared in 10mM Tris-HCl (pH adjusted to 7.0) and DMSO, respectively. The stock solution of **2** (50 mM) was prepared in 10 mM Tris-HCl and the pH adjusted to 7.0. For cocrystallization experiments, the inhibitors were diluted to 4 mM in the concentrated protein solution and incubated at 4 °C with shaking overnight.

Kinetic Parameters. The DHQase activity was assayed by monitoring the increase in A_{234} accompanying conversion of 3-dehydroquinate to 3-dehydroshikimate.[27] Assays were performed at 25 °C using 50 mM Tris-acetate buffer, pH 7.0, in a total volume of 1 mL. Reactions were initiated by addition of enzyme (0.011, 0.4, and 5 μg for the enzymes from *S. coelicolor*, *M. tuberculosis*, and *H. pylori*, respectively). Kinetic parameters were obtained by varying the concentration of 3-dehydroquinate (synthesized as previously described[23]) over the range from 50 to 400 μM in the presence and absence of inhibitors. The concentrations of solutions of substrate were calculated on the basis of the limiting change in A_{234} on addition of 1 μg of *S. coelicolor* DHQase, taking into account that the equilibrium constant for formation of 3-dehydroshikimate is 15.[9]

The values of K_m and V_{max} were obtained by fitting the data to the Michaelis−Menten equation by nonlinear regression using Microcal (Northampton, MA) Origin software. Within a set of inhibition studies, the errors in these parameters were within 10% of the stated value. Inhibition constants were derived from the changes in K_m in the presence of inhibitor. The values of k_{cat} were calculated using 16.5, 18.0, and 20.6 kDa for the subunit molecular masses from the enzymes from *S. coelicolor*, *M. tuberculosis*, and *H. pylori*, respectively.

Whole Cell Antimicrobial Assay. Three cell lines were used, TG1 (wild-type *E. coli* strain), AB2848 (-DHQase strain), and AB2848 with a plasmid encoded (pet19) *H. pylori* DHQase. Samples were taken from plates containing the cell lines and

cultured with shaking in L-broth at 37 °C for 4 h. The cells were pelleted by centrifugation, washed three times (to remove any contaminating aromatic amino acids), and finally resuspended in PBS equivalent to the original culture volume. Three types of media were used, minimal media, minimal media plus 1 mM shikimate, and L-broth. Media was supplemented with 200 μg/mL ampicillin and 0.1 mM IPTG for the plasmid containing cell line, and 10 μL of each PBS-suspended cell line was added to 2.5 mL of media together with the **3** suspended in 12.5 μL of DMSO (final concentration 50 μg/mL, 0.145 mM) and incubated at 37 °C for ~16 h. After incubation, 300 μL was taken from each sample and the absorbance was measured at 595 nm.

Crystallization and Data Collection. Crystallization experiments were carried out using the sitting drop vapor diffusion method with a drop size of 1 μL of protein mixed with 1 μL of precipitant. Initial crystallization conditions were identified using commercial sparse matrix screens and optimized by linear screening of conditions. Octahedral-shaped crystals of *H. pylori* DHQase in complex with **3** were grown using 1 M Na acetate, 0.1 M imidazole-HCl, pH 8.0, appeared after 48 h, and grew to a maximum size of 0.3 × 0.3 × 0.3 mm over 1 week. For X-ray data collection, the crystals were transferred to a solution of mother liquor + 20% glycerol to act as a cryoprotectant and then frozen at 100 K in a stream of gaseous nitrogen. These crystals were found to diffract to 2.5-Å resolution in house, using a rotating anode source (Nonius FR591) and a MacScience DIP2000 detector. Initial indexing of the data showed that the crystals were cubic with unit cell dimensions $a = 130.5$ Å, space group $F23$, with one protein monomer per asymmetric unit. Data were integrated and scaled using the HKL suite [28] and were used for the initial structure solution. Subsequently, a 1.5 Å resolution data set was collected on beamline 9.6 at the Daresbury SRS, which was used for the refinement of the structure.

Irregular hexagonal bipyramid crystals of the *H. pylori* DHQase **1** complex were grown from 30% 1,4 butanediol, 0.1 M Na acetate, pH 4.5. The butanediol in the crystallization conditions proved to be a good cryoprotectant; therefore, crystals were directly flash frozen at 100 K for data collection. The crystals were found to diffract to 3.1-Å resolution on beamline 9.5 at the Daresbury SRS and indexed in a primitive trigonal space group with unit cell dimensions $a = b = 103.86$ Å, $c = 217.53$ Å, $\alpha = \beta = 90°$, $\gamma = 120°$. Analysis of the systematic absences showed that the reflection condition $h = 3n$ was obeyed; the data were therefore processed in the $P3_1$ space group. Data were integrated and scaled using the HKL suite of programs. Calculation of the Matthews coefficient[29] suggested the presence of one dodecamer per asymmetric unit for this space group. Data processing statistics for the inhibitors structures are summarized in Table 1.

Structure Solution and Refinement. The structure of *H. pylori* DHQase−**3** complex was solved by the molecular replacement method using the program EPMR.[30] A polyalanine model of the type II DHQase from *M. tuberculosis* (PDB[8] 2DHQ) was used as the search model, and the top ranked solution had a correlation coefficient of 33.8% and an *R* factor of 55.4%.

Weighted phases were calculated from the molecular replacement solution using SIGMAA from the CCP4 suite of programs.[31] These phases were subsequently modified using DM[32] to decrease the amount of model bias arising from the MR process. The figure-of-merit-weighted $2F_o - F_c$ maps were clearly traceable, allowing 80% of the main chain to be built, and side chain density was visible for 75% of the residues. Ten percent of reflections were set aside for free *R*-factor calculation. Restrained refinement was carried out using REFMAC5[33] followed by manual alteration of the model using QUANTA (Accelrys, San Diego, CA). After two rounds of refinement and model building, clear $F_o - F_c$ density was visible in the active site region corresponding to **3**. A model of the ligand was prepared using Insight II (Accelrys) and was docked into the electron density using the X-LIGAND module within the QUANTA package.

The 1.5-Å data were used in the subsequent rounds of refinement and model building, with the same free *R*-factor set of reflections retained and extended to the higher resolution. Water molecules were added either manually using the X-SOLVATE module in QUANTA or automatically using ARP.[34] Molecules of imidazole from the crystallization media and glycerol from the cryoprotectant solution were also added to the model. In the final stages of refinement, restrained anisotropic B-factor refinement was applied as implemented in REFMAC5.[35]

The structure of the *H. pylori* DHQase−**1** complex was solved by molecular replacement using the program AMoRe[36] with the trimer unit of the *H. pylori* DHQase−**3** structure as the search model and using data between 12- and 4.0-Å resolution. AMoRe was run to find four trimers within the asymmetric unit; 12 peaks of identical height were found in the rotation search. The final MR solution had a correlation coefficient of 69.9% and *R*-factor 34.4% after rigid body refinement. The *H. pylori* DHQase−**1** model was refined with REFMAC applying strict 12-fold NCS restraints relating to each monomer within the asymmetric unit. A 12-fold averaged $F_o - F_c$ map was used to fit **1** with the X-LIGAND module within QUANTA.

For comparison with the other *H. pylori* structures, the coordinate file and corresponding structure factors for the type II DHQase from *H. pylori* (PDB code 1J2Y) were downloaded from the Protein Data Bank. Ligand and water molecules were removed from the model, rigid body refinement was carried out using REFMAC5,[33] and weighted $2F_o - F_c$ and $F_o - F_c$ electron density maps were calculated. The active site difference density was correctly identified as **2**; this was docked into the difference density map using X-LIGAND within QUANTA. Five rounds of refinement and model building were carried out in which four peptides in loops were flipped, a number of side chain rotamers were corrected, and 40 water molecules were added.

The final models were analyzed using PROCHECK[37] and were shown to have good geometry with 98% of residues in the allowed region of the Ramachandran plot. The refinement statistics for each structure are summarized in Table 1. The DHQase structures have been deposited in the protein data bank (PDB) with accession codes 2C4V for the citrate complex, 2C4W for the AH9095 complex, and 2C57 for the FA1 complex.

Acknowledgment. We thank the Biotechnology and Biological Sciences Research Council for studentships to D.A.R. and K.A.S. D.A.R. received support from the GlaxoSmithKline Action TB program. We thank Prof. C Abell for the gift of FA1 and useful discussions.

References

(1) Abell, C. Enzymology and molecular biology of the shikimate pathway. *Comprehensive Natural Products Chemistry*; Elsevier: Amsterdam, 1999; pp 573−607.
(2) Bentley, R. The shikimate pathway—A metabolic tree with many branches. *Crit. Rev. Biochem. Mol. Biol.* **1990**, *25*, 307−384.
(3) Roberts, C. W.; Roberts, F.; Lyons, R. E.; Kirisits, M. J.; Mui, E. J.; et al. The shikimate pathway and its branches in apicomplexan parasites. *J. Infect. Dis.* **2002**, *185 Suppl 1*, S25−36.
(4) Hoiseth, S. K.; Stocker, B. A. D. Aromatic-dependent *Salmonella-typhimurium* are non-virulent and effective as live vaccines. *Nature* **1981**, *291*, 238−239.
(5) Ivins, B. E.; Welkos, S. L.; Knudson, G. B.; Little, S. F. Immunization against anthrax with aromatic compound-dependent (Aro-) mutants of *Bacillus-anthracis* and with recombinant strains of *Bacillus-subtilis* that produce anthrax protective antigen. *Infection Immunity* **1990**, *58*, 303−308.
(6) Simmons, C. P.; Hodgson, A. L. M.; Strugnell, R. A. Attenuation and vaccine potential of aroQ mutants of *Corynebacterium pseudotuberculosis*. *Infection Immunity* **1997**, *65*, 3048−3056.
(7) Parish, T.; Stoker, N. G. The common aromatic amino acid biosynthesis pathway is essential in *Mycobacterium tuberculosis*. *Microbiology* **2002**, *158*, 3069−3077.
(8) Gourley, D. G.; Shrive, A. K.; Polikarpov, I.; Krell, T.; Coggins, J. R.; et al. The two types of 3-dehydroquinase have distinct structures but catalyze the same overall reaction. *Nat. Struct. Biol.* **1999**, *6*, 521−525.

(9) Kleanthous, C.; Deka, R.; Davis, K.; Kelly, S. M.; Cooper, A.; et al. A comparison of the enzymological and biophysical properties of two distinct classes of dehydroquinase enzymes. *Biochem. J.* **1992**, *282*, 687−695.
(10) Harris, J. M.; Kleanthous, C.; Coggins, J. R.; Hawkins, A.; Abell, C. Different mechanistic and stereochemical courses for the reactions catalysed by type I and type II dehydroquinases. *J. Chem. Soc., Chem. Commun.* **1993**, *1993*, 1080−1081.
(11) Chaudhuri, S.; Duncan, K.; Graham, L. D.; Coggins, J. R. Identification of the active-site lysine residues of two biosynthetic 3-dehydroquinases. *Biochem. J.* **1991**, *275*, 1−6.
(12) Harris, J. M.; Gonzalez-Bello, C.; Kleanthous, C.; Hawkins, A. R.; Coggins, J. R.; et al. Evidence from kinetic isotope studies for an enolate intermediate in the mechanism of type II dehydroquinases. *Biochem. J.* **1996**, *319*, 333−336.
(13) Frederickson, M.; Parker, E. J.; Hawkins, A.; Coggins, J. R.; Abell, C. Selective inhibition of type II dehydroquinases. *J. Org. Chem.* **1999**, *64*, 2612−26134.
(14) Frederickson, M.; Roszak, A. W.; Coggins, J. R.; Lapthorn, A. J.; Abell, C. (1*R*,4*S*,5*R*)-3-Fluoro-1,4,5-trihydroxy-2-cyclohexene-1-carboxylic acid: The fluoro analogue of the enolate intermediate in the reaction catalysed by type II dehydroquinases. *Org. Biomol. Chem.* **2004**, *2*, 1592−1596.
(15) Le Sann, C.; Gower, M. A.; Abell, A. D. Inhibitors of type I and II dehydroquinase. *Mini Rev. Med. Chem.* **2004**, *4*, 747−756.
(16) Roszak, A. W.; Robinson, D. A.; Krell, T.; Hunter, I. S.; Fredrickson, M.; et al. The structure and mechanism of the type II dehydroquinase from *Streptomyces coelicolor*. *Structure* **2002**, *10*, 493−503.
(17) Frederickson, M.; Roszak, A. W.; Coggins, J. R.; Lapthorn, A. J.; Abell, C. (1*R*,4*S*,5*R*)-3-Fluoro-1,4,5-trihydroxy-2-cyclohexene-1-carboxylic acid: The fluoro analogue of the enolate intermediate in the reaction catalyzed by type II dehydroquinases. *Org. Biomol. Chem.* **2004**, *2*, 1592−1596.
(18) Gonzalez-Bello, C.; Lence, E.; Toscano, M. D.; Castedo, L.; Coggins, J. R.; et al. Parallel solid-phase synthesis and evaluation of inhibitors of Streptomyces coelicolor type II dehydroquinase. *J. Med. Chem.* **2003**, *46*, 5735−5744.
(19) Toscano, M. D.; Frederickson, M.; Evans, D. P.; Coggins, J. R.; Abell, C.; et al. Design, synthesis and evaluation of bifunctional inhibitors of type II dehydroquinase. *Org. Biomol. Chem.* **2003**, *1*, 2075−2083.
(20) Lee, B. I.; Kwak, J. E.; Suh, S. W. Crystal structure of the type II 3-dehydroquinase from *Helicobacter pylori*. *Proteins—Struct. Funct. Genet.* **2003**, *51*, 616−617.
(21) Kwak, J. E.; Lee, J. Y.; Han, B. W.; Moon, J. J.; Sohn, S. H.; et al. Crystallization and preliminary X-ray crystallographic analysis of type II dehydroquinase from *Helicobacter pylori*. *Acta Crystallogr. D Biol. Crystallogr.* **2001**, *57*, 279−280.
(22) Bottomley, J. R.; Clayton, C. L.; Chalk, P. A.; Kleanthous, C. Cloning, sequencing, expression, purification and preliminary characterization of a type II dehydroquinase from *Helicobacter pylori*. *Biochem. J.* **1996**, *319*, 559−565.
(23) Evans, L. D. B.; Roszak, A. W.; Noble, L. J.; Robinson, D. A.; Chalk, P. A.; et al. Specificity of substrate recognition by type II dehydroquinases as revealed by binding of polyanions. *Febs Lett.* **2002**, *530*, 24−30.
(24) Harris, J. M.; Watkins, W. J.; Hawkins, A.; Coggins, J. R.; Abell, C. Comparison of the substrate specificity of type I and type II dehydroquinases with 5-deoxy and 4,5-dideoxy-dehydroquinic acid. *J. Chem. Soc., Perkin Trans.* **1996**, *1996*, 2371−2377.
(25) Madge, D.; Wishart, G.; Dolaman, M.; Maunder, P. Bissulfonamides as inhibitors of the dehydroquinate synthase enzyme AroB and the Type II dehydroquinase enzyme AroQ. In *Expert Opinion upon Therapeutic Patents*; Arrow Therapeutics Ltd.: London, 2001; pp 1797−1799.
(26) Carpenter, E. P.; Hawkins, A. R.; Frost, J. W.; Brown, K. A. Structure of dehydroquinate synthase reveals an active site capable of multistep catalysis. *Nature* **1998**, *394*, 299−302.
(27) White, P. J.; Young, J.; Hunter, I. S.; Nimmo, H. G.; Coggins, J. R. The purification and characterization of 3-dehydroquinase from *Streptomyces coelicolor*. *Biochem. J.* **1990**, *265*, 735−738.
(28) Otwinowski, Z.; Minor, W. Processing of X-ray diffraction data collected in oscillation mode. *Methods Enzymol.* **1997**, *276*, 307−326.
(29) Matthews, B. W. Solvent content of protein crystals. *J. Mol. Biol.* **1968**, *33*, 491−497.
(30) Kissinger, C. R.; Gehlhaar, D. K.; Fogel, D. B. Rapid automated molecular replacement by evolutionary search. *Acta Crystallogr. Sect. D-Biol. Crystallogr.* **1999**, *55*, 484−491.
(31) CCP4 The CCP4 suite—Programs for protein crystallography. *Acta Crystallogr. Sect. D-Biol. Crystallogr.* **1994**, *50*, 760−763.
(32) Cowtan, K. DM: An automated procedure for phase improvement by density modification. In *Joint CCP4 and ESF-EACBM Newsletter on Protein Crystallography*, 1994; pp 34−38.
(33) Murshudov, G. N.; Vagin, A. A.; Dodson, E. J. Refinement of macromolecular structures by the maximum-likelihood method. *Acta Crystallogr. Sect. D-Biol. Crystallogr.* **1997**, *53*, 240−255.
(34) Lamzin, V. S.; Wilson, K. S. Automated refinement of protein models. *Acta Crystallogr. Sect. D-Biol. Crystallogr.* **1993**, *49*, 129−147.
(35) Murshudov, G. N.; Vagin, A. A.; Lebedev, A.; Wilson, K. S.; Dodson, E. J. Efficient anisotropic refinement of macromolecular structures using FFT. *Acta Crystallogr. Sect. D-Biol. Crystallogr.* **1999**, *55*, 247−255.
(36) Navaza, J. AMoRe—An automated package for molecular replacement. *Acta Crystallogr. Sect. A* **1994**, *50*, 157−163.
(37) Laskowski, R. A.; Macarthur, M. W.; Moss, D. S.; Thornton, J. M. Procheck—A program to check the stereochemical quality of protein structures. *J. Appl. Crystallogr.* **1993**, *26*, 283−291.
(38) Cruickshank, D. W. J. Remarks about protein structure precision. *Acta Crystallogr. Sect. D-Biol. Crystallogr.* **1999**, *55*, 583−601.
(39) Thompson, J. D.; Higgins, D. G.; Gibson, T. J. Clustal-W—Improving the sensitivity of progressive multiple sequence alignment through sequence weighting, position-specific gap penalties and weight matrix choice. *Nucleic Acids Res.* **1994**, *22*, 4673−4680.
(40) Gouet, P., Courcelle, E., Stuart, D. I.; Metoz, F. ESPript: Multiple sequence alignments in PostScript. *Bioinformatics* **1999**, *15*, 305−308.

JM0505361